Pointing a Ground Antenna at a Spinning Spacecraft Using Conscan–Simulation Results

A. Mileant and T. Peng
Telecommunications Systems Section

This article presents the results of an investigation of ground antenna pointing errors which are caused by fluctuations of the receiver AGC signal due to thermal noise and a spinning spacecraft. Transient responses and steady-state errors and losses are estimated using models of the digital Conscan (conical scan) loop, the FFT, and antenna characteristics. Simulation results are given for the on-going Voyager mission and for the upcoming Galileo mission, which includes a spinning spacecraft. The simulation predicts a 1-sigma pointing error of 0.5 to 2.0 mdeg for Voyager, assuming an AGC loop SNR of 35 to 30 dB with a scan period varying from 128 to 32 sec, respectively. This prediction is in agreement with the DSS 14 antenna Conscan performance of 1.7 mdeg for 32-sec scans as reported in earlier studies. The simulation for Galileo predicts 1-mdeg error with a 128-sec scan and 4-mdeg with a 32-sec scan under similar AGC conditions.

I. Introduction

In order to reduce the pointing error of the DSN ground antennas, a technique called Conscan has been successfully used for many years. In Conscan, angle tracking is accomplished by scanning the antenna around boresight in a circular pattern with constant angular offset, called the scan radius. The basic theory of Conscan is given in [1]. In the present implementation of the Conscan technique, the downlink signal is processed by a Fast Fourier Transform (FFT) algorithm.

In this article, the impact of downlink AGC fluctuations due to thermal noise and a spinning spacecraft on the pointing error of a ground antenna is investigated. In Section II the Conscan process is modeled as a digital phase-locked loop combined with the FFT algorithm. This analysis is subdivided into the following sections:

A. Modeling the downlink signal

B. Algorithm for estimating the pointing error

C. Impact of spacecraft motion on the pointing error

D. Impact of AGC SNR on the pointing error

E. Conscan closed-loop model

F. Pointing jitter and pointing loss

G. Transient response

Section III presents a computer simulation of the Conscan model. Predicted performance in terms of steady-state and transient responses, as well as time constants, are given as a function of loop gain, scan period, and signal-to-noise ratio. Specific topics discussed are:

II. Analysis

A. Modeling of the Downlink Signal

The Conscan technique uses AGC samples of the ground receiver in order to estimate the ground antenna pointing angle. In general, the AGC samples are perturbed by several causes: by deliberate ground antenna scanning about its boresight, by thermal noise in the AGC loop, by spacecraft antenna mispointing, and by other factors such as changes in gain and weather conditions.

In our analysis, we first will assume that the AGC loop operates at very high SNR so that the AGC fluctuations due to thermal noise can be neglected. The effect of thermal noise will be addressed later in this analysis.

Let P_c be the average carrier power reaching the ground receiver when the receiving antenna is perfectly pointed and let $\beta(t)$ be the instantaneous pointing offset of the receiving antenna. Then, with imperfect ground antenna pointing, the signal power reaching the ground receiver will be

$$r(t) = P_c + l_r[\beta(t)] \qquad \text{(dBm)} \qquad (1)$$

Where $l_r(\cdot)$ represents the power loss due to pointing offset of the receiving antenna (a negative number in dB).

When a spinning spacecraft is tracked, $r(t)$ will experience periodic fluctuations of the form

$$\sum_{i=1}^{M} K_i \cos(\omega_i t + \phi_i) \qquad (2)$$

where K_i represents the maximum power deviation about the mean (in units of dB) at the frequency ω_i (which will be some multiple of the spacecraft's spin rate). Both K_i and ω_i are determined by the spacecraft's antenna gain pattern and dynamics.

The instantaneous pointing offset of the ground antenna, according to [1], can be expressed by the following equation

$$\beta(t) = \left[R^2 + \theta_e^2 + \theta_x^2 + 2R(\theta_x \cos \omega_T t + \theta_e \sin \omega_T t)\right]^{1/2}$$
$$(3)$$

where

R = scan radius

θ_e = pointing error in elevation angle

θ_x = pointing error in cross-elevation angle

ω_T = $2\pi/T$, where T is the Conscan period

For small pointing offsets, the pointing loss due to *ground* antenna offset can be approximated by the least square fitting of a parabola to the antenna gain pattern. In our analysis we let

$$l_r(\beta) = K_r \beta^2 \qquad \text{(dB)} \qquad (4)$$

where K_r is a constant.

Combining the effects of scanning the ground antenna and a spinning spacecraft, the downlink AGC signal will be of the form

$$r(t) = P_c + l_r[\beta(t)] + \sum K_i \cos(\omega_i t + \phi_i) \qquad (5)$$

In Conscan implementation, the received AGC signal power, $r(t)$, is sampled every I seconds and stored in a one-dimensional array. Inserting Eqs. (3) and (4) into Eq. (5) and making $T = IN$ and $t = Ij$, we obtain the downlink AGC signal at the *sampling instants*, namely,

$$r_j = \left[P_c + K_r(R^2 + \theta_x^2 + \theta_e^2)\right]$$
$$+ 2K_r R\left[\theta_x \cos\left(\frac{2\pi j}{N}\right) + \theta_e \sin\left(\frac{2\pi j}{N}\right)\right]$$
$$+ \left[\sum K_i \cos(\omega_i Ij + \phi_i)\right] \qquad (6)$$

where the subscript j refers to the jth sample of a scan cycle, $j = 0, \ldots, N-1$. Subscript i refers to the ith contribution to the signal. The variables ϕ_i are random phases generated by a spinning spacecraft (for example, by its wobble and nutation). In general the spacecraft's spin rate is faster than the scan rate and should not be a multiple of the later (otherwise the scan rate must be changed accordingly). In this case, the phases ϕ_i will be approximately uniformly distributed in the $\{0, 2\pi\}$ interval. P_c as well as K_i ($i = 1, \ldots, M$), R, θ_x, and θ_e are

assumed to be constant during many scan periods. Equation (6) can be written as follows

$$r_j = P + c_j + n_j \tag{7}$$

where P represents the terms contained in the first pair of square brackets of Eq. (6), which correspond to the dc component; c_j represents the terms contained in the second pair of square brackets, which include the signal variation produced by scanning the ground antenna in a circular pattern, where θ_x and θ_e are the pointing errors that we want to correct; and n_j represents the terms inside the third pair of square brackets, which are the signal fluctuations produced by the spinning spacecraft.

B. Algorithm for Estimating the Pointing Error

In the present implementation of the Conscan technique, at the end of a scan period, N AGC samples are Fourier transformed with an FFT algorithm. The antenna pointing errors are estimated from the *first component* of the FFT (see Fig. 1). Since the FFT is just a fast implementation of the Discrete Fourier Transform, we will apply the theory of DFT to estimate the impact of a spinning spacecraft on the Conscan signal.

Let D^k be the kth component of the Discrete Fourier Transform operator defined by

$$D^k(r) = \left(\frac{1}{N}\right) \sum_{j=0}^{N-1} r_j \left[\cos\left(\frac{2\pi k j}{N}\right) + i \sin\left(\frac{2\pi k j}{N}\right) \right] \tag{8}$$

We rewrite this equation as follows

$$D^k(r) \doteq R(k) = R_R(k) + i R_I(k) \tag{9}$$

where $R_R(k)$ and $R_I(k)$ are the real and imaginary parts of the kth component of the DFT, $k = 0, 1, \ldots, N-1$. Carrying out the above DFT operation on Eq. (6) we obtain

Real part

$$R_R(k) = \begin{cases} P + N_R(0) & \text{for } k = 0 \\ K_r R \theta_x + N_R(1) & \text{for } k = 1 \\ N_R(k) & \text{otherwise} \end{cases} \tag{10}$$

Imaginary part

$$R_I(k) = \begin{cases} N_I(0) = 0 & \text{for } k = 0 \\ K_r R \theta_e + N_I(1) & \text{for } k = 1 \\ N_I(k) & \text{otherwise} \end{cases} \tag{11}$$

where P equals the sum of terms in the first pair of square brackets in Eq. (6), whose value is of *no interest* in our analysis. As we see from Eqs. (10) and (11), θ_x and θ_e can be estimated from $R_R(1)$ and $R_I(1)$, namely,

$$\widehat{\theta}_x = \frac{R_R(1)}{K_r R}$$

$$\widehat{\theta}_e = \frac{R_I(1)}{K_r R} \tag{12}$$

$N_R(1)$ and $N_I(1)$ result from the modulation of the downlink signal produced by a spinning spacecraft. Since the above terms superimpose to the terms containing θ_x and θ_e (see Eqs. 10 and 11), they have the effect of an additive noise which corrupts the estimation of the ground antenna pointing error. In what follows, the impact of $N_R(1)$ and $N_I(1)$ on $\widehat{\theta}_x$ and $\widehat{\theta}_e$ will be investigated.

C. Impact of a Spinning Spacecraft on the Pointing Error

We begin by taking the DFT on n_j, the terms inside the third pair of square brackets in Eq. (6), namely

$$D^k(n) = D^k \left[\sum K_i \cos(\omega_i I j + \phi_i) \right]$$

$$\doteq N(k) = N_R(k) + i N_I(k) \tag{13}$$

where $N_R(k)$ and $i N_I(k)$ are the real and imaginary parts of $N(k)$. Using Eqs. (A-21) and (A-23) of the Appendix we obtain

$$N_R(1) = \left(\frac{1}{2N}\right) \sum_{\text{all } i} K_i \sin \gamma_{0i}$$

$$\times \left[\cos \phi_i (C_{1i} + C_{2i}) - \sin \phi_i (C_{3i} + C_{4i}) \right]$$

$$\tag{14}$$

$$N_I(1) = \left(\frac{1}{2N}\right) \sum_{\text{all } i} K_i \sin \gamma_{0i}$$

$$\times \left[\cos \phi_i (C_{3i} - C_{4i}) - \sin \phi_i (-C_{1i} + C_{2i}) \right]$$

where

$$C_{1i} = \frac{\cos\gamma_{1i}}{\sin\gamma_{3i}} \qquad C_{2i} = \frac{\cos\gamma_{2i}}{\sin\gamma_{4i}}$$

$$C_{3i} = \frac{\sin\gamma_{1i}}{\sin\gamma_{3i}} \qquad C_{4i} = \frac{\sin\gamma_{2i}}{\sin\gamma_{4i}}$$

$$\gamma_{0i} = \frac{\pi I N}{T_i}$$

$$\gamma_{1i} = \pi\left[\frac{I(N-1)}{T_i} + \frac{1}{N}\right] \qquad \gamma_{2i} = \pi\left[\frac{I(N-1)}{T_i} - \frac{1}{N}\right]$$

$$\gamma_{3i} = \pi\left[\frac{I}{T_i} - \frac{1}{N}\right] \qquad \gamma_{4i} = \pi\left[\frac{I}{T_i} + \frac{1}{N}\right]$$

$$(15)$$

When ϕ_i are uniformly distributed, the evaluation of $N_R(1)$ and $N_I(1)$ is straightforward. It is shown in the Appendix that $N_R(1)$ and $N_I(1)$ are processes with zero mean, and variances (expressed in dB²) of

$$\text{var}\{N_R(1)\} \doteq \sigma_{Rs}^2 = \left(\frac{1}{8N^2}\right)\sum_{\text{all }i}(K_i\sin\gamma_{0i})^2$$

$$\times \left[(C_{1i} + C_{2i})^2 + (C_{3i} + C_{4i})^2\right]$$

$$\text{var}\{N_I(1)\} \doteq \sigma_{Is}^2 = \left(\frac{1}{8N^2}\right)\sum_{\text{all }i}(K_i\sin\gamma_{0i})^2$$

$$\times \left[(C_{3i} - C_{4i})^2 + (-C_{1i} + C_{2i})^2\right]$$

$$(16)$$

In order to gain more insight into the operation of the Conscan algorithm, we can think of the FFT as digital filtering. In this context, we can compute the contribution to the variances σ_{Rs}^2 and σ_{Is}^2 in terms of the ith modulation component of a spinning spacecraft and the FFT's transfer function, namely

$$\sigma_{Rsi}^2 = F_R^2(i)(K_i\sin\gamma_{0i})^2$$

$$(17)$$

$$\sigma_{Isi}^2 = F_I^2(i)(K_i\sin\gamma_{0i})^2$$

where the transfer functions for the real and imaginary parts are obtained from Eq. (16), namely

$$F_R^2(i) = \left(\frac{1}{8N^2}\right)\left[(C_{1i} + C_{2i})^2 + (C_{3i} + C_{4i})^2\right]$$

$$(18)$$

$$F_I^2(i) = \left(\frac{1}{8N^2}\right)\left[(C_{3i} - C_{4i})^2 + (-C_{1i} + C_{2i})^2\right]$$

Figure 2 shows the frequency response of $F^2(f) = F_R^2(f) + F_I^2(f)$, the magnitude squared of the first FFT's component. Note that the transfer function of the FFT processing is periodic. The period equals I, which is the AGC sampling time (usually 1 sec). So, the frequencies f_i ($f_i = \omega_i/2\pi$), which are multiples of $1/I$, hurt the Conscan estimator the most. Minima of $F^2(f)$ are 23 dB below the maximum. Note that $F^2(f)$ has nulls at multiples of $1/T$. Figure 2 also shows the ratio of $F_R^2(f)/F_I^2(f)$ versus frequency.

With this information about the properties of the transfer function of the FFT algorithm, we can select the Conscan period T so as to minimize the impact of unwanted frequencies, ω_i. Ideally, we would like to have freedom in selecting both the AGC sampling time I, and the Conscan period T, so that the unwanted frequencies will fall at the nulls or where the FFT's frequency response is minimal. For example, we would like to select the sampling time I so that the following condition is met

$$\frac{\omega_1}{2\pi} \approx \left(\frac{n}{I} + 0.5\right)$$

where ω_1 is the most significant component of the spin rate and n is an integer.

D. Effect of AGC SNR on the Pointing Error

Again let P_c be the nominal carrier power reaching the ground receiver and SNR be the signal-to-noise ratio in the AGC loop. Then the noise variance in the AGC loop will be $\sigma_N^2 = P_c/SNR$. The instantaneous *signal plus thermal noise* power of the jth AGC sample will be

$$r_j = 20.0\log\left(\sqrt{P_c} + V_{Nj}\right)$$

$$(19)$$

where V_{Nj} is a zero mean Gaussian random variable with variance σ_N^2. The standard deviation of the r_j sample (assuming that only thermal noise is present) will be approximately

$$\sigma_r \approx 20.0 \log \left[\frac{\left(\sqrt{P_c} + \sigma_N \right)}{\sqrt{P_c}} \right] \quad \text{(dB)} \quad (20)$$

It is shown in the Appendix that the variances of the real and imaginary parts at the output of the FFT in terms of the variance of the AGC thermal noise are

$$\sigma_{Rt}^2 = \sigma_{It}^2 = \frac{\sigma_r^2}{2N} \quad \text{(dB}^2) \quad (21)$$

The overall variances at the output of the FFT will be simply the sum of the individual variances due to spacecraft spin and receiver thermal noise, namely

$$\sigma_R^2 = \sigma_{Rs}^2 + \sigma_{Rt}^2$$
$$\sigma_I^2 = \sigma_{Is}^2 + \sigma_{It}^2 \quad (22)$$

where σ_{Rs}^2 and σ_{Is}^2 are given by Eq. (16) and σ_{Rt}^2 and σ_{It}^2 by Eq. (21).

E. Conscan Closed-Loop Model

So far we have discussed the open-loop estimation of the pointing errors. In order to proceed with this analysis, we define the *closed-loop pointing errors* in cross-elevation and elevation as follows

$$\phi_{x(n+1)} \doteq \theta_{xn} - \widehat{\theta}_{xn}$$
$$\phi_{e(n+1)} \doteq \theta_{en} - \widehat{\theta}_{en} \quad (23)$$

where $\widehat{\theta}_x$ and $\widehat{\theta}_e$ are the Conscan estimates of the pointing offsets θ_x and θ_e, respectively. We will treat all of the above angles as *continuous* variables of time and model the DFT as an analog multiplication and integration. This approach is allowable because the AGC sampling time I is much smaller than the Conscan update time, $T = NI$. Being in closed-loop, we substitute ϕ_x for θ_x and ϕ_e for θ_e in the third term of Eq. (6) and rewrite that term in vector notation as follows:

$$2 K_r R \left[\cos \frac{2\pi t}{N} \quad \sin \frac{2\pi t}{N} \right] \begin{bmatrix} \phi_x(t) \\ \phi_e(t) \end{bmatrix} \quad (24)$$

The DFT algorithm (modeled here as an analog operation) multiplies this input by the vector

$$\left[\cos \frac{2\pi t}{N} \quad i \sin \frac{2\pi t}{N} \right]$$

integrates from 0 to N, and divides the result by N. This operation is represented schematically below.
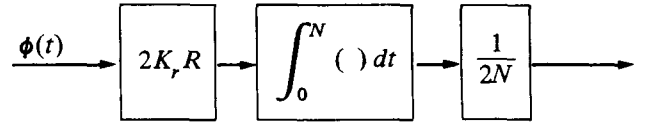
where

$$\phi(t)^T = [\phi_x(t) \quad \phi_e(t)] \quad (25)$$

The factor of 1/2 results from the multiplication of a cosine by a cosine and a sine by a sine. Double frequency terms are integrated to zero. Thus, the DFT operation for a large N can be modeled as an integrate-and-dump device with the following transfer function in the hybrid s/z-domain.
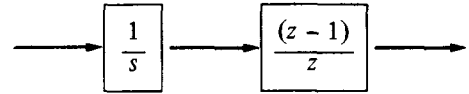
In the feedback path of the Conscan loop, the estimated errors in antenna pointing are scaled down by a factor G, and the antenna pointing corrections, $\widehat{\theta}_x$ and $\widehat{\theta}_c$, are obtained. This corresponds to the following set of difference equations

$$\widehat{\theta}_{xn} = \widehat{\theta}_{x(n-1)} + G \widehat{\phi}_{xn}$$
$$\widehat{\theta}_{en} = \widehat{\theta}_{e(n-1)} + G \widehat{\phi}_{en} \quad (26)$$

where $\widehat{\phi}_x$ and $\widehat{\phi}_e$ are the estimates of ϕ_x and ϕ_e, respectively. The subscript n indicates the nth scan period. In Fig. 3 the above difference equation has the following z-domain transfer function (summer)

$$S(z) \doteq \frac{\widehat{\theta}(z)}{\widehat{\phi}(z)} = \frac{z}{(z-1)} \quad (27)$$

Because $\widehat{\theta}_x$ and $\widehat{\theta}_e$ are modeled as continuous variables of time, we need to convert the discrete variables $\widehat{\theta}_x(z)$ and $\widehat{\theta}_e(z)$ to their continuous counterparts, namely, we need a Digital-to-

Analog converter (D/A) in the feedback path of our loop model. The transfer function for the D/A is

$$\frac{(1 - e^{-sN})}{s} \tag{28}$$

where $e^{-sN} \doteq z^{-1}$.

By combining the above elements into a block diagram, Fig. 3 is obtained. Now the above hybrid s/z-loop model may be converted to a z-domain model. Neglecting for the moment the noise term $N(z)$, we see by inspection of Fig. 3 that

$$X'(s) = \frac{2K_r R\theta(s)}{s} - X'(z) \frac{\left[\frac{(z-1)}{z}\right]G}{(Ns^2)} \tag{29}$$

Taking the z-transform of Eq. (29) and simplifying, we obtain

$$X'(z) = 2K_r R \left[\frac{\theta(s)}{s}\right]^* - X'(z) \frac{G}{(z-1)} \tag{30}$$

where the asterisk denotes the z-transform operation.

With this transformation, Fig. 3 has the equivalent block diagram of Fig. 4, which is entirely in the z-plane. From Fig. 4 we see that the overall Conscan open loop transfer function is

$$G(z) = \frac{Y(z)}{X(z)} = \frac{G}{(z-1)} \tag{31}$$

and the closed-loop transfer function is

$$H(z) = \frac{Y(z)}{\left[\frac{\theta(s)}{s}\right]^*} = \frac{G(z)}{[1 + G(z)]} = \frac{G}{[z + (G-1)]} \tag{32}$$

Having obtained $H(z)$, we now need the following integral

$$I_1 = \frac{1}{i2\pi} \oint H(z) H(z^{-1}) \frac{dz}{z} \tag{33}$$

Using Table III of [2], it is found that

$$I_1 = \frac{G}{(2-G)} \tag{34}$$

Assuming then the noise sample $N_{n+1}(1)$ is independent of $N_n(1)$ for all n, it can be shown that the steady-state closed-loop variances of the pointing error are

$$\sigma_x^2 = \frac{I_1 \sigma_R^2}{(K_r R)^2} \quad \text{(in units of } R^2\text{)}$$

$$\sigma_e^2 = \frac{I_1 \sigma_I^2}{(K_r R)^2} \quad \text{(in units of } R^2\text{)} \tag{35}$$

where σ_R^2 and σ_I^2 are the open-loop variances at the output of the FFT and are given by Eq. (22).

Before moving to the next topic it should be noted that the transfer function $H(z)$ of the Conscan loop, Eq. (32), has a single pole at $z = 1 - G$. The stability criterion requires that $|1 - G| < 1$ in order for the pole to remain inside the unit circle. This puts an upper bound on the loop gain which has to be less than 2. Control theory predicts that the Conscan loop will have a bounded steady-state error to a ramp or velocity input. In practice, the velocity components of the pointing axis are compensated by predicts, while Conscan compensates for step pointing errors.

F. Pointing Jitter and Pointing Loss

Equation (4) relates the ground antenna pointing loss to the pointing error. In order to estimate the closed-loop pointing loss, we substitute ϕ_x for θ_x and ϕ_e for θ_e in Eq. (3). Then we insert Eq. (3) into Eq. (4) and integrate over one scan period to obtain

$$1_r = K_r\left(R^2 + \phi_x^2 + \phi_e^2\right) \tag{36}$$

where ϕ_x and ϕ_e are random variables with zero mean (assuming a step input) and the variance is given by Eq. (35). Invoking the central limit theorem, we can assume that the closed-loop pointing errors ϕ_x and ϕ_e have a Gaussian distribution. Being derived from quadrature processes, they are mutually independent. With the above assumptions, we take the expected value of Eq. (36) and obtain the closed-loop pointing loss, L, namely

$$L \doteq \mathbf{E}\{1_r\}$$

$$= K_r\left[R^2 + \mathbf{E}(\phi_x^2) + \mathbf{E}(\phi_e^2)\right] \tag{37}$$

$$= K_r(R^2 + \sigma_x^2 + \sigma_e^2) \quad \text{(dB)} \tag{38}$$

G. Transient Response

Let $\theta_{xn} = \theta_{x1}$ and $\theta_{en} = \theta_{e1}$ for all n. Inserting Eq. (26) in Eq. (23) and taking the expected value, it can be shown that

$$\phi_{xn} = \theta_{x1} r^{(n-1)}$$

$$\phi_{en} = \theta_{e1} r^{(n-1)}$$ (39)

or, in vector notation

$$\boldsymbol{\phi}_n = \boldsymbol{\theta}_1 r^{(n-1)}$$ (40)

where

$$r \doteq 1 - G \qquad (0 < r < 1)$$

We now define the time constant, τ, as the time in seconds that it takes for pointing error ϕ_n to decay to the value of θ_1/e, where e is the base of the natural logarithm. Solving for the number of Conscan periods, $n-1$, necessary for θ_1 to decrease by $1/e$ and for the corresponding τ, it can be shown that

$$n - 1 = -\frac{1}{\ln(r)}$$ (41)

and

$$\tau = -\frac{T}{\ln(r)}$$ (42)

Figure 5 depicts typical τ values for DSN antennas.

III. Computer Simulation

A. Simulation Model

A computer program named CONSCAN.FOR using an FFT subroutine was written in order to check the above analysis. In our simulation, values typical for the Voyager and the Galileo missions were used.

In the actual implementation of the Conscan algorithm at the DSN stations the FFT computation can start at any time inside a Conscan period. In order to account in our simulation for this time shift between the FFT reference point and AGC samples, the estimates of the pointing error were computed with the following modification to Eq. (12)

$$\text{MAG} = \frac{\left[R_R^2(1) + R_I^2(1)\right]^{1/2}}{(K_r R)}$$ (43)

$$\text{ANG} = \tan^{-1}\left[\frac{R_I(1)}{R_R(1)}\right] + \gamma$$ (44)

where γ represents the relative angle offset between the AGC table of the antenna scan cycle. In Eq. (44), a four-quadrant arc tangent is computed. Finally, the estimates of the pointing error are computed

$$\theta_x = \text{MAG} \cdot \cos(\text{ANG})$$

$$\theta_e = \text{MAG} \cdot \sin(\text{ANG})$$ (45)

This revised estimation algorithm for the pointing error shows a slight crosscoupling between θ_x and θ_e. In this simulation, in order to mimic more closely an actual antenna, the antenna pointing corrections were done gradually in an interval of eight to ten samples with a slight overshoot before the final point.

Figures 6 through 9 display the results of the simulation. The variances of the pointing error were averaged over 550 Conscan periods. The computer-simulated results agree very closely with the equations derived in this analysis.

The following values were used in the simulation: $K_r R^2 = 0.1$ dB for both the 64- and 70-m antennas; scan period $T = 32$, 64, and 128 sec; and sampling time $I = 1$ sec. Conscan loop gain $G = 0.05, 0.3$, and 0.6. $P_c = -145$ dBm, and the AGC loop SNR was between 20 and 50 dB.

For the Galileo spacecraft, the effect of the spin on the transmitted signal was modeled as follows (see Eq. 2)

$$\Sigma K_i \cos(\omega_i t + \phi_i) = K_t \alpha^2 \qquad \text{(dB)}$$ (46)

where α, the effective offset from the correct pointing of the spacecraft antenna, is defined as

$$\alpha(t) = \Big[\alpha_1^2 + \alpha_2^2 + \alpha_3^2 + 2\alpha_1\alpha_2 \cos(\omega_1 t + \phi_1)$$

$$+ 2\alpha_1\alpha_3 \cos(\omega_2 t + \phi_2)$$

$$+ 2\alpha_2\alpha_3 \cos(\omega_3 t + \phi_3)\Big]^{1/2}$$ (47)

Here

α_1 = combined pointing error due to Earth-fitting error, spacecraft/Earth drift, and attitude determination error

α_2 = pointing error due to nutation

α_3 = pointing error due to wobble, mechanical and electrical misalignments

In our simulation we made $K_1 = 2\alpha_1\alpha_2 = 1$ dB, $K_2 = 2\alpha_1\alpha_3 = 0.2$ dB, and $K_3 = 2\alpha_2\alpha_3 = 0.2$ dB. Other variables are defined as follows: ω_1 = nutation spin rate, ω_2 = wobble spin rate, $\omega_3 \doteq \omega_1 - \omega_2$. The following values were assumed: wobble period $T_1 = 19.048$ sec (nominal or low spin rate); nutation period $T_2 = 14.583$ sec $(T_2 \approx T_1/1.3)$; $K_t = -77.5$ dB/deg^2 (curve fit to Galileo X-band antenna gain pattern).

B. Simulation Results—Choice of Loop Gain and Scan Period

From Figs. 6 through 9 we can make the following observations:

Increasing the gain G decreases the time constant and, hence, the lock-up time, although it increases the pointing fluctuations and pointing loss (Figs. 6 and 7). This fact suggests the following operational strategy: choose a large gain value during lock-up, and a small gain value during tracking. This strategy has been successfully used with the Real-Time Combiner of the DSN Baseband Assembly.

Increasing the scan period decreases the pointing jitter (Figs. 8 and 9). This effect is especially pronounced for Galileo which has larger pointing jitter due to spacecraft spin. Increasing the scan period, however, also slows down the pointing correction process.

C. Simulation Versus Actual Performance for Voyager

The simulation result is comparable with the observed antenna Conscan performance in supporting Voyager. Figure 8 predicts a 1-sigma pointing error of 0.5 (128-sec scan) to 1.5 mdeg (32-sec scan) for Voyager, assuming thermal noise 35 dB below the carrier level in a 1-Hz AGC loop. In [3] the Conscan performance of the DSS 14 64-m antenna in pointing Voyager over 5 days in 1987 is reported (see Fig. A5 in [3]), with statistics given in Fig. A6 for individual scans with a 32-sec period. The standard deviation reported is 1.7 mdeg, in good agreement with our simulation result.

D. Predicted Performance for Galileo

In the case of Galileo, the Conscan performance is affected by both thermal noise in the receiver and the wobble and nutation reflected in the spacecraft signal. Figure 9 indicates that the thermal noise is the dominant effect when the AGC loop SNR is lower than about 30 dB. But the wobble and nutation effect dominates when the AGC is higher than 30 dB. As a result, the pointing error can be reduced by increasing the AGC SNR below 30 dB, but not beyond 30 dB.

It should be noted that the Conscan period must be chosen carefully in order to avoid harmonic relationship with the wobble and nutation processes. In case both wobble and nutation are present, the scan period of 64 sec should be avoided because its frequency, 0.0156 Hz, is very close to the difference between the wobble and nutation frequencies, 0.0162 Hz. Abnormal pointing errors were indeed observed in simulation.

E. Simulation Results Versus Predicted Performance

Simulation results give slightly more conservative values for the pointing error variances than the ones predicted by the closed-form solution, Eq. (35). The possible reasons are (a) in our simulation, the lock-up transients have partially effected the statistics of the pointing error; and (b) an error in the phase offset γ in Eq. (44) was deliberately introduced in our simulation in order to approximate the actual pointing imperfections.

The discrepancy can be illustrated with two cases. For Voyager, with $T = 32$ sec, $SNR = 35$ dB and $G = 0.6$, the standard deviation of the pointing error is 0.6 mdeg according to the closed-form solution and 1 mdeg according to the simulation. For Galileo, with the same conditions, the standard deviation of the pointing error is 2 mdeg according to the closed-form solution and 3 mdeg according to the simulation.

IV. Conclusion

A model has been developed to analyze and simulate the performance of DSN antenna Conscan as affected by the fluctuations in the receiver AGC signal. The effects of the receiver thermal noise and of the spinning spacecraft were analyzed and simulated. The simulation results agreed well with the observed performance of the DSS 14 antenna supporting Voyager. The simulation results show a standard deviation of 1.5 mdeg at X-band with 32-sec scan for a 35-dB AGC SNR. Observed performance at DSS 14 [3] for Voyager under similar AGC SNR conditions was about 1.7 mdeg for individual scans.

The simulation results suggested that the Conscan loop gain and the scan period can be chosen to optimize the pointing performance. A higher gain and a shorter scan period can reduce pointing acquisition time at the beginning of the track. A lower gain and a longer scan period can reduce the standard deviation of pointing jitters, and, therefore, the loss, during track.

The simulation result for Galileo indicated higher pointing jitter than Voyager because of the additional effect of spacecraft wobble and nutation on the ground receiver AGC signal. The spacecraft effect is dominated by the ground receiver thermal noise effect for the AGC SNR below 30 dB and becomes dominant when the SNR is above 30 dB. Figure 9 predicts a relative constant pointing error in the latter region. This region is typical for Galileo support when the carrier signal level is at least −155 dBm.

The Conscan pointing error for Galileo under such conditions was between 1 mdeg (128-sec scan) and 4 mdeg (32-sec scan). The corresponding losses versus the standard deviations of pointing errors are given in Fig. 10.

It was noted that the choice of a Conscan period for Galileo must avoid harmonic relationships with the Galileo wobble and nutation frequencies. The results of the analysis indicated that the 64-sec scan should not be used for Galileo when both wobble and nutation are present.

Acknowledgment

References

[1] J. E. Ohlson and M. S. Reid, *Conical-Scan Tracking with the 64-m Diameter Antenna at Goldstone*, JPL Technical Report 32-1605, Jet Propulsion Laboratory, Pasadena, California, October 23, 1976.

[2] E. I. Jury, *Theory and Applications of the Z-Transform Method*, Malabar, Florida: R. E. Krieger Publishing Co., 1982.

[3] C. N. Guiar et al., "DSS 14 Antenna Calibration for GSSR/VLA Saturn Radar Experiments," *TDA Progress Report 42-93*, vol. January–March 1988, Jet Propulsion Laboratory, Pasadena, California, pp. 309–337, May 15, 1988.
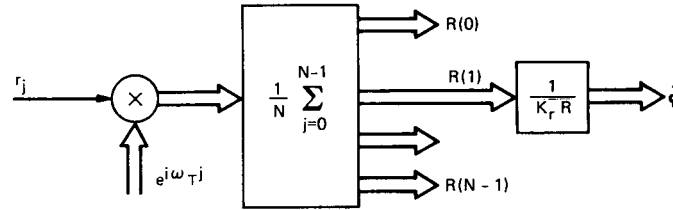
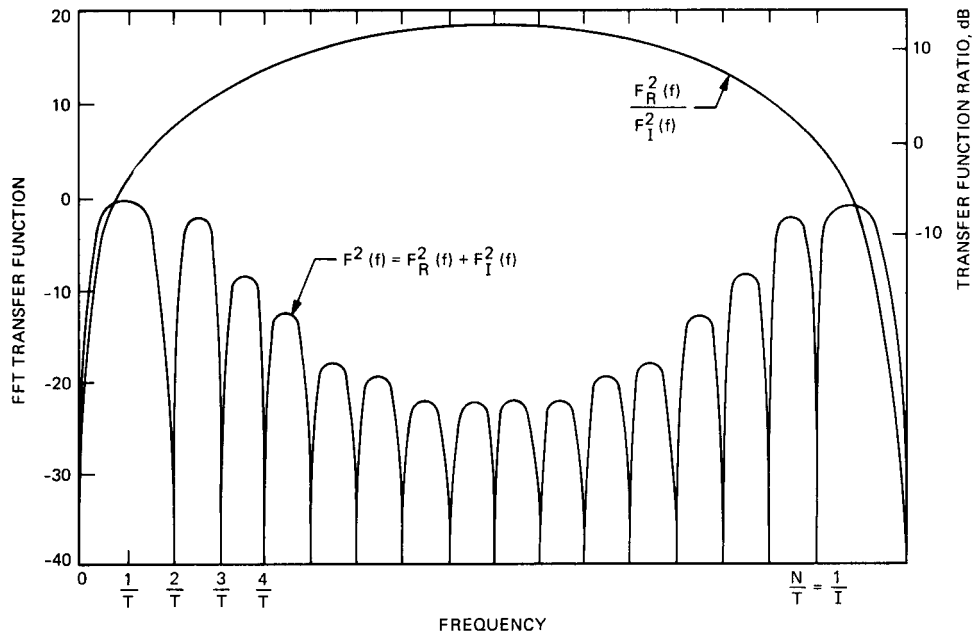Fig. 1. Open-loop estimation of the pointing errors.

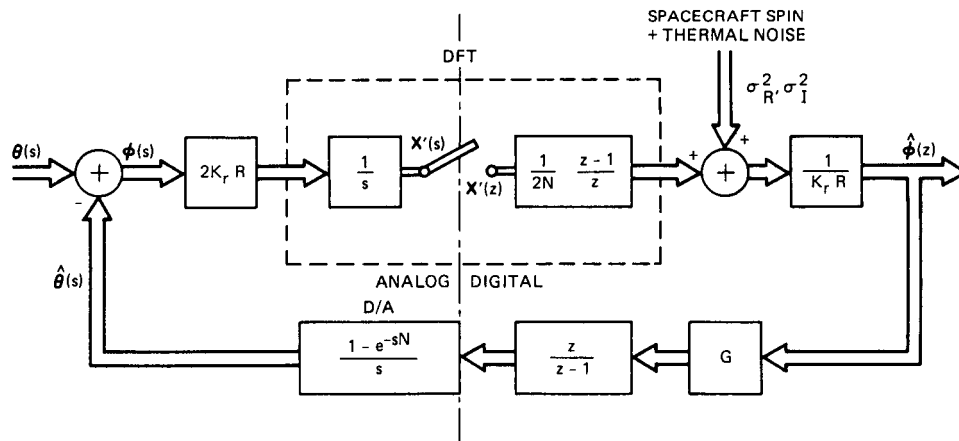Fig. 2. Total (Real + Imaginary) FFT Transfer Function and Transfer Function Ratio (Real/Imaginary).

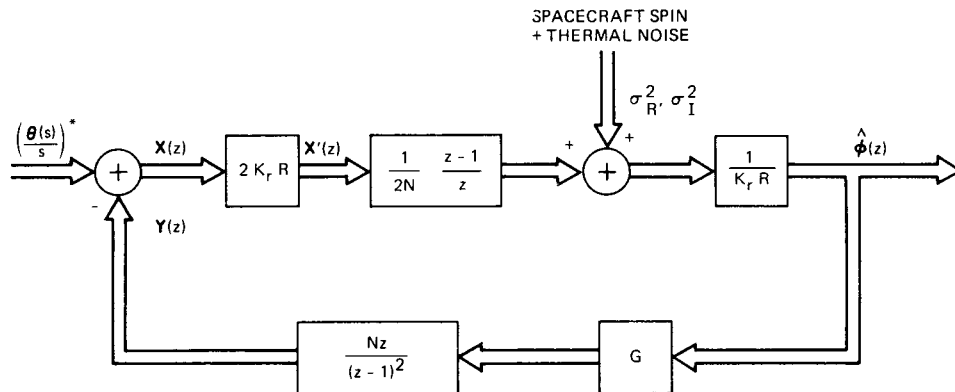Fig. 3. Closed-loop hybrid s/z-domain model of the Conscan process.
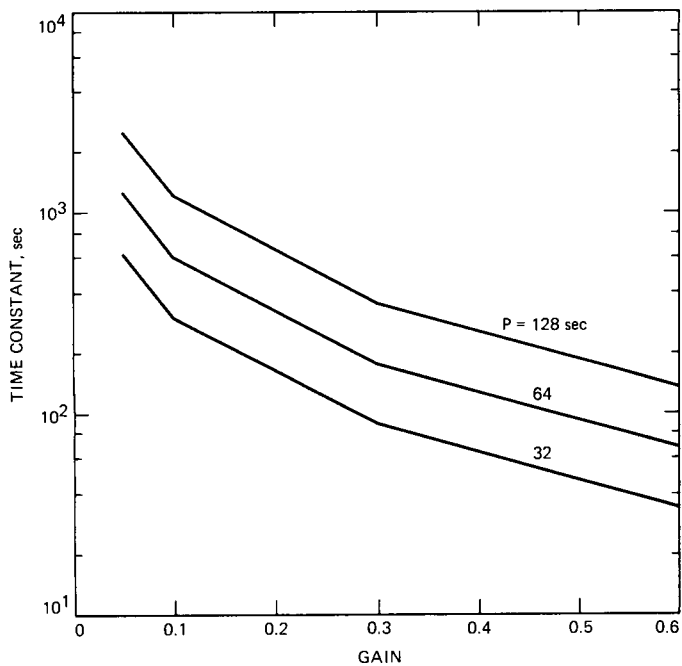
Fig. 4. Z-domain model of the Conscan process.
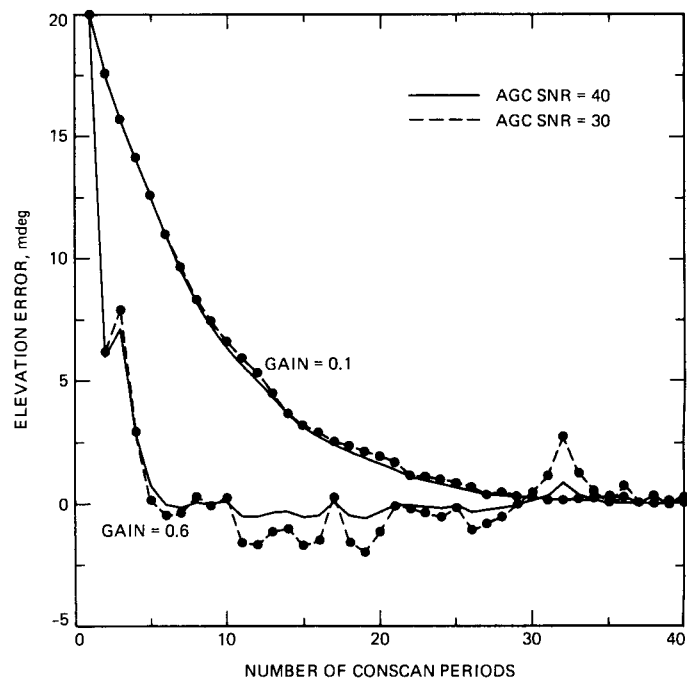

Fig. 5. Time constant versus closed-loop gain.

Fig. 6. Transient response of pointing error simulation for Voyager spacecraft (a typical case).
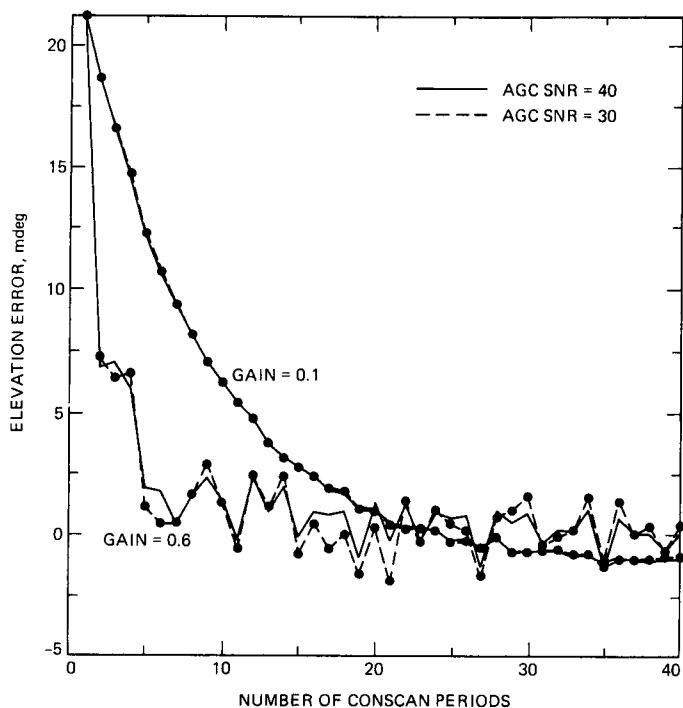
Fig. 7. Transient response of pointing error simulation for Galileo spacecraft (a typical case).
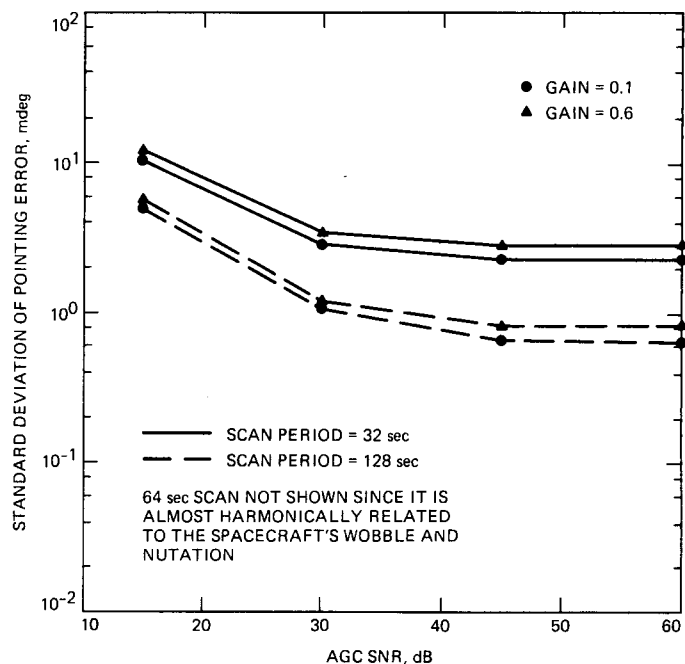

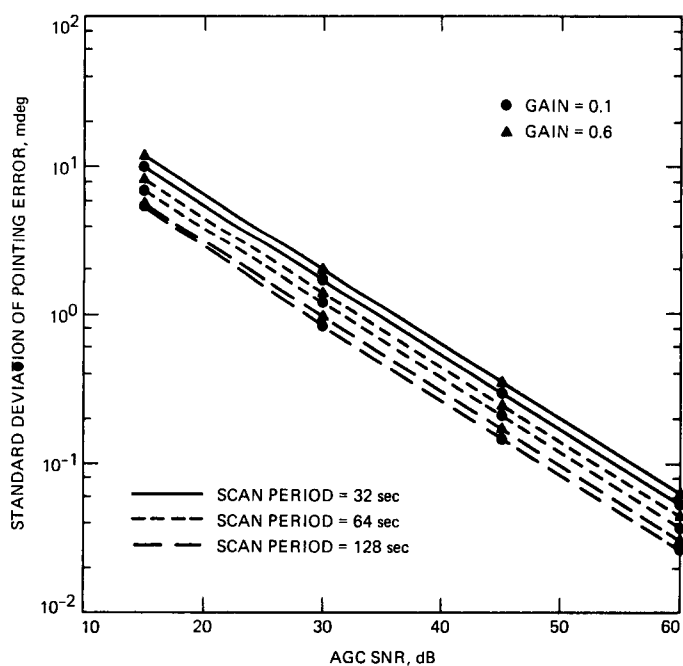Fig. 9. Steady-state pointing error versus AGC SNR simulation for Galileo spacecraft.

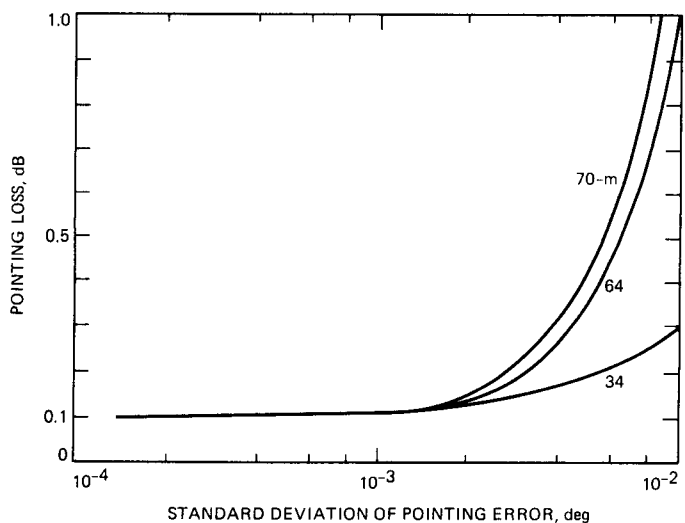Fig. 8. Steady-state pointing error versus AGC SNR simulation for Voyager spacecraft.

Fig. 10. Pointing loss versus standard deviation of the pointing error at X-band for 34-, 64-, and 70-m antennas. Nominal pointing loss due to Conscan = 0.1 dB.

Appendix A

Derivation of the Mean Value and Variance at the Output of DFT

Let D^k be the Discrete Fourier Transform operator defined as follows

$$D^k(S) = \left(\frac{1}{N}\right) \sum_{j=0}^{N-1} S_i \left[\cos\left(\frac{2\pi kj}{N}\right) + i\sin\left(\frac{2\pi kj}{N}\right)\right] \quad (A\text{-}1)$$

$$\doteq R(k) = R_R(k) + iR_I(k) \quad (A\text{-}2)$$

where $R_R(k)$ and $R_I(k)$ are the real and imaginary parts of $R(k)$, respectively.

We want to find the mean value and the variance of $R(k)$ for the following three cases

$$S_i = \begin{cases} S & (A\text{-}3) \\ S\cos\left(\frac{2\pi Ij}{T_i}\right) & \text{so that } K = \frac{NI}{T_i} \text{ is an integer} \quad (A\text{-}4) \\ S\cos\left(\frac{2\pi Ij}{T_i} + \phi_i\right) & \text{for any nonrandom } T_i \text{ and random } \phi_i, \text{ uniformly distributed} \quad (A\text{-}5) \end{cases}$$

where S is a random variable assumed to be constant during one Conscan period. And we define

$$E\{S\} \doteq \mu_S \quad \text{and} \quad \text{var}\{S\} \doteq \sigma_S^2 \quad (A\text{-}6)$$

$$E\{D^k(r)\} \doteq \mu(k) = \mu_R(k) + i\mu_I(k) \quad (A\text{-}7a)$$

$$E\{D^k(r)^2\} - \mu(k)^2 \doteq \sigma^2(k) = \sigma_R^2(k) + \sigma_I^2(k) \quad (A\text{-}7b)$$

A. $S_i = S$

Using Eq. (A-1) it is easy to see that

$$\mu_R(k) = \begin{cases} \mu_S & \text{for } k = 0 \\ 0 & \text{otherwise} \end{cases} \quad (A\text{-}8)$$

$$\mu_I(k) = 0 \quad \text{for all } k \quad (A\text{-}9)$$

$$\sigma_R^2(k) = \begin{cases} \sigma_S^2 & \text{for } k = 0 \\ 0 & \text{otherwise} \end{cases} \quad (A\text{-}10)$$

$$\sigma_I^2(k) = 0 \quad \text{for all } k \quad (A\text{-}11)$$

B. S_i Periodic as Defined by Eq. (A-4)

With $K = NI/T_i = $ integer, we have

$$S\cos\left(\frac{2\pi Ij}{T_i}\right) = S\cos\left(\frac{2\pi Kj}{N}\right) \quad (A\text{-}12)$$

Using Eq. (A-1) we obtain

$$\mu_R(k) = \begin{cases} \dfrac{\mu_S}{2} & \text{for } k = K \\ 0 & \text{otherwise} \end{cases} \quad (A\text{-}13)$$

$$\mu_I(k) = 0 \quad \text{for all } k \quad (A\text{-}14)$$

$$\sigma_R^2(k) = \begin{cases} \dfrac{\sigma_S^2}{4} & \text{for } k = K \\ 0 & \text{otherwise} \end{cases} \quad (A\text{-}15)$$

$$\sigma_I^2(k) = 0 \quad \text{for all } k \quad (A\text{-}16)$$

C. S_i Periodic With Any Period Length and Phase Shift

Let

$$S_i = S\cos\left(\frac{2\pi Ij}{T_i}\right) + \phi_i \quad (A\text{-}17)$$

$$= S\left[\cos\phi_i \cos\left(\frac{2\pi Ij}{T_i}\right) - \sin\phi_i \sin\left(\frac{2\pi Ij}{T_i}\right)\right] \quad (A\text{-}18)$$

Using Eq. (A-1) for the real part, we let $\omega_1 = 2\pi I/T_i$ and $\omega_2 = 2\pi k/N$. Then

$$R_R(k) = \left(\frac{S}{N}\right) \sum_{j=0}^{N-1} \left[\cos\phi_i \cos\omega_1 j - \sin\phi_i \sin\omega_1 j\right] \cos\omega_2 j$$

$$= \left(\frac{S}{2N}\right) \sum_{j=0}^{N-1} \left[\cos\phi_i \, \text{Real}\left\{e^{i(\omega_1-\omega_2)j} + e^{i(\omega_1+\omega_2)j}\right\}\right.$$

$$\left. - \sin\phi_i \, \text{Imag.}\left\{e^{i(\omega_1+\omega_2)j} + e^{i(\omega_1+\omega_2)j}\right\}\right]$$

$$= \left(\frac{S}{2N}\right)\left[\cos\phi_i \, \text{Real}\left\{\frac{1-e^{i(\omega_1-\omega_2)N}}{1-e^{i(\omega_1-\omega_2)}} + \frac{1-e^{i(\omega_1+\omega_2)N}}{1-e^{i(\omega_1+\omega_2)}}\right\}\right.$$

$$\left. - \sin\phi_i \, \text{Imag.}\left\{\frac{1-e^{i(\omega_1-\omega_2)N}}{1-e^{i(\omega_1-\omega_2)}} + \frac{1-e^{i(\omega_1+\omega_2)N}}{1-e^{i(\omega_1+\omega_2)}}\right\}\right]$$

(A-19)

But

$$e^{\pm i\omega_2 N} \equiv 1$$

and

$$\frac{1-e^{i\omega_1 N}}{1-e^{i(\omega_1 \pm \omega_2)}} = e^{i[(\omega_1(N-1)\mp\omega_2]} \frac{\sin\left(\frac{\omega_1 N}{2}\right)}{\sin\left[\frac{(\omega_1 \pm \omega_2)}{2}\right]}$$

(A-20)

Using Eq. (A-20) in Eq. (A-19) and simplifying we obtain

$$R_R(k) = \left(\frac{S}{2N}\right) \sin\gamma_0 \left[\cos\phi_i (C_1 + C_2) - \sin\phi_i (C_3 + C_4)\right]$$

(A-21)

where

$$C_1 = \frac{\cos\gamma_1}{\sin\gamma_3} \qquad\qquad C_2 = \frac{\cos\gamma_2}{\sin\gamma_4}$$

$$C_3 = \frac{\sin\gamma_1}{\sin\gamma_3} \qquad\qquad C_4 = \frac{\sin\gamma_2}{\sin\gamma_4}$$

$$\gamma_0 = \frac{\pi IN}{T_i}$$

$$\gamma_1 = \pi\left[\frac{I(N-1)}{T_i} + \frac{k}{N}\right] \qquad \gamma_2 = \pi\left[\frac{I(N-1)}{T_i} - \frac{k}{N}\right]$$

$$\gamma_3 = \pi\left[\frac{I}{T_i} - \frac{k}{N}\right] \qquad\qquad \gamma_4 = \pi\left[\frac{I}{T_i} + \frac{k}{N}\right]$$

(A-22)

Note that C_i and γ_i $(i = 1, \ldots, 4)$ are functions of the variable k. Repeating the above steps for the imaginary part of $R(k)$ we obtain

$$R_I(k) = \left(\frac{S}{2N}\right) \sin\gamma_0 \left[\cos\phi_i (C_3 - C_4) - \sin\phi_i (-C_1 + C_2)\right]$$

(A-23)

Assuming that ϕ_i is uniformly distributed in the interval $\{0, 2\pi\}$, we obtain

$$\mu_R = \mu_I = 0 \qquad\qquad \text{for all } k \qquad (A\text{-}24)$$

$$\sigma_R^2(k) = \sigma_S^2 \left(\frac{1}{8N^2}\right) (\sin\gamma_0)^2$$

$$\times \left[(C_1 + C_2)^2 + (C_3 + C_4)^2\right] \qquad (A\text{-}25)$$

$$\sigma_I^2(k) = \sigma_S^2 \left(\frac{1}{8N^2}\right) (\sin\gamma_0)^2$$

$$\times \left[(C_3 - C_4)^2 + (-C_1 + C_2)^2\right] \qquad (A\text{-}26)$$

where again σ_S^2 is the variance of S and other variables are defined in Eq. (A-22).

259

D. White Noise

Assuming that the variance of each voltage sample due to thermal noise is σ_v^2, the variance of the sum of N samples will be $N\sigma_v^2$. The FFT algorithm performs the N complex sums and divides the result by N. Hence the total variance of the complex FFT output will be

$$\sigma_T^2 = \sigma_v^2 N \left(\frac{1}{N}\right)^2 = \frac{\sigma_v^2}{N} \tag{A-27}$$

Since in our implementation of the DFT the output is split into its real and imaginary parts, the variance of each of them will be one-half of σ_v^2.

C-2